Proceedings of the 2005 IEEE
Engineering in Medicine and Biology 27th Annual Conference
Shanghai, China, September 1-4, 2005

Computer-Aided Diagnosis Scheme for Detection of Unruptured Intracranial Aneurysms in MR Angiography

Y. Uchiyama[1], H. Ando[2], R. Yokoyama[1], T. Hara[1], H. Fujita[1], T. Iwama[2]
[1]Department of Intelligent Image Information, Graduate School of Medicine, Gifu University, Japan
[2]Department of Neurosurgery, Graduate School of Medicine, Gifu University, Japan

Abstract— **The detection of unruptured intracranial aneurysms is a major subject in magnetic resonance angiography (MRA) images. However, it is difficult for radiologists to detect small aneurysms on the maximum intensity projection (MIP) images, because adjacent vessels overlap with the aneurysm. The purpose of this study was to develop an automated computerized detection of aneurysms in order to assist radiologists' interpretation as a "second opinion." The vessels were first segmented from background by use of gray-level thresholding and region growing technique. The gradient concentrate (GC) filter was then applied to the segmented vessels for enhancement of aneurysm. The initial aneurysm candidate was identified in the GC image with a gray level threthold. For removal of false positives (FPs), we determined three features, i.e., size, sphericity, and mean value of GC image in each of the candidate regions. Finally, the rule-based schemes with these features and quadratic discriminant analysis were applied for distinction between aneurysms and FPs. The sensitivity of our method for detection of aneurysms was 100% (7/7) with 1.85 FPs per patient. With our computerized scheme, all aneurysms were detected correctly with low FP rates, and would be useful in assisting radiologists for identifying correct aneurysms and for reducing the interpretation time.**

Keywords—**Computer-aided diagnosis (CAD), unruptured intracranial aneurysm, magnetic resonance angiography (MRA)**

I. Introduction

The detection and management of unruptured intracranial aneurysms is a major subject in magnetic resonance angiography (MRA) images, because most of subarachnoid haemorrhage arises from rupture of an intracranial aneurysm [1]. Between 3.6 and 6% of population harbor an intracranial aneurysm. The ruptured rate of asymptomatic aneurysms was thought to be 1-2% per annum [1]. However, it is difficult for radiologists to detect small aneurysms in MRA image, because some adjacent vessels overlap with the aneurysm on maximum intensity projection (MIP) image. Therefore, the purpose of this study was to develop a computer-aided diagnosis (CAD) scheme for detection of intracranial aneurysms on MRA images in order to assist radiologists' interpretation as a "second opinion."

In the previous study for detection of intracranial aneurysms in MRA image, Arimura *et al.* [2]-[3] developed a method for detection of aneurysms based on the 3D selective enhancement filter. They reported the sensitivity for detection of aneurysms was 100% with 2.4 false positives (FPs) per patients by use of a database consisted of 29 cases with 36 aneurysms and 31 non-aneurysms cases. Rohde *et al.* [4] developed a method based on Fourier analysis to provide an objective factor for assessment of the risk of rupture. Their quantitative assessment with 45 unruptured intracranial aneurysms and 46 ruptured intracranial aneurysms showed surface irregularities in 78% of unruptured and 42% of unruptured intracranial aneurysms.

In this study, we developed an automated computerized method for detection of aneurysms based on gradient concentrate (GC) filer. Since a new method with low false positive rates is required for clinical application, we investigated the usefulness of features obtained from GC filter.

This work was supported by a grant for the "Intellectual Cluster Creation Project" from the Ministry of Education, Culture, Sports, Science and Technology, Japan.

II. Methodology

A. Clinical Cases

We selected twenty MRA studies, which were acquired on a 1.5 T magnetic imaging scanner (Signa Excite Twin Speed 1.5T; GE Medical Systems, Milwaukee, WI) by use of a 3D time-of-flight technique in the Gifu University Hospital (Gifu, Japan). The 3D MRA images included slices ranged from 50 to 140. The axial image matrix size was 256 × 256 pixels with the pixel size ranged from 0.625 mm to 0.78 mm. The slice thickness ranged from 0.5 mm to 1.2 mm.

All original 3D MRA images were converted to isotropic volume data by using linear interpolation, where each of the volume data was 400 × 400 × 200 voxels with a voxel size of 0.5 mm. Twenty clinical cases were used in this study, which included 7 abnormal cases with 7 aneurysms (diameter, 2.3 to 3.5 mm; mean, 2.8 mm) and 13 normal cases. The locations of all aneurysms were determined by one of authors (H.A.). 4 aneurysms were located at middle cerebral artery, 2 aneurysms at internal carotid artery, and 1 aneurysm at posterior cerebral artery.

B. Segmentation of Vessel Regions

To limit the search spaces to the aneurysms, and to avoid generating FPs due to the outside of vessel regions, the vessel regions were first segmented automatically. Because the maximum and minimum values of the voxels were different in each of twenty 3D MRA images, the linear gray-level transform was applied to the 3D MRA images so that minimum value was zero and the voxel values higher than 99% of the cumulative histogram were changed as a maximum value of 1024. To segment vessels regions from background, the gray-level thresholding was applied to the 3D MRA images with a threshold level of 700, which was selected empirically. With this method, the regions of large vessels were segmented correctly. However, it is difficult to segment small vessels, because the voxel values in small vessels were low intensities, and extra-vessel structures were segmented together with lower threshold level. To tackle this problem, we used a region growing technique, which start with the regions of segmented large vessels as "seed" points and grow regions by appending to each seed point when a value in neighboring voxels was larger than 500. Fig.1 shows the result of our method. Most of the vessels were segmented correctly.

C. Determination of Initial Aneurysm Candidates

For enhancement of aneurysms and suppression of vessels, we used a GC filter based on iris filter [5]-[7], which was designed to enhance rounded convex regions by measuring the degree of convergence of the gradient vectors around a point of interest. However, a difficulty of GC filters in the application to 3D image processing is time-consuming. Therefore, we used a simplified version of GC filter, and the GC filter was applied to the vessel regions segmented from background. The simplified GC filter used in this study was defined by

$$GC(p) = \frac{1}{M}\sum_{R}\cos\theta_j \,. \qquad (1)$$

The output value of GC filter at the point of interest p was computed within the regions of a sphere with radius R at the center of p. R was given as 5 pixels in this study. M is the number of voxels when the gradient magnitude located at j was larger than zero. The angle θ is the angle between the direction vector from p to j and a gradient direction vector located at j. The gradient magnitude and gradient direction were calculated by the first-order difference filter.

For identification of initial aneurysm candidates, the gray-level thresholding technique with a threshold level of 50 voxel value was applied to the image obtained by GC filter. The threshold level was selected empirically. We determined the initial aneurysm candidates as the "islands" whose size was larger than 10 voxels, because the threshold level was gives as the smallest value so that the regions of all aneurysms could be detected, and thus a lot of small "islands" were also detected.

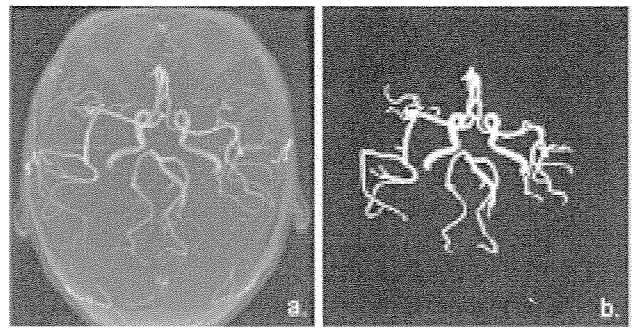

Fig.1. Illustration of (a) MIP image of original MRA slices and (b) segmented vessel image.

D. Removal of False Positives

For removal of FPs, we used three image features, i.e., size, the degree of sphericity, and mean value of GC image. The size was gives as the number of voxels in the regions of initial aneurysm candidate. The size may be useful a feature for eliminating FPs, because the sizes of some FPs were smaller or larger than those of aneurysms. The degree of sphericity, which was defined by the fraction of the overlap volume of the candidate with the sphere having the same volume as the candidate, may be also useful a feature for distinction between vessels and aneurysms, because some FPs were line-like or more irregular compared with aneurysms. However, the degree of sphericity used in this study can not find small dot-like objects such as aneurysms, because it is difficult to quantify the shape of surface accurately when the size of candidate was small. Thus, we used mean value of GC image in the candidate regions as another feature. Some FPs may be eliminated by simple rules with these three features. Therefore, the rule-base scheme with these three features was used as the first step for removal of FPs.

In the final stage of our CAD scheme, quadratic discriminant analysis [8] with three features was carried out for further removal of FPs. The quadratic discriminant analysis generates a decision boundary that optimally partitions the feature space spanned by three features into two class, i.e., aneurysm class and FP class. The decision boundary for quadratic discriminant analysis was a quadratic surface given by discriminant function. The output value of discriminant function indicates the likelihood of aneurysm. Thus, we can classify the aneurysm candidates into true-positive class and FP class by partitioning the feature space with a threshold level of discriminant function. By changing the threshold level, we can determine the performance for detection of aneurysms with our CAD scheme.

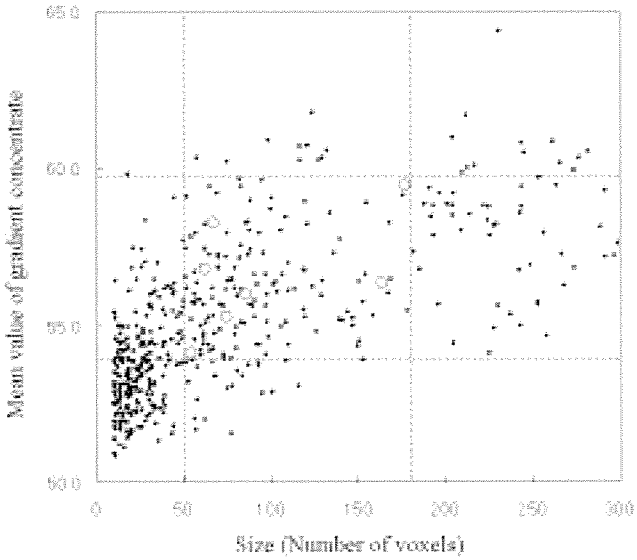

Fig. 2. Relationship between size and degree of sphericity in each of initial candidate regions (aneurysms: circles; false positive: dots). The dotted lines indicate the thresholds for removal of false positives.

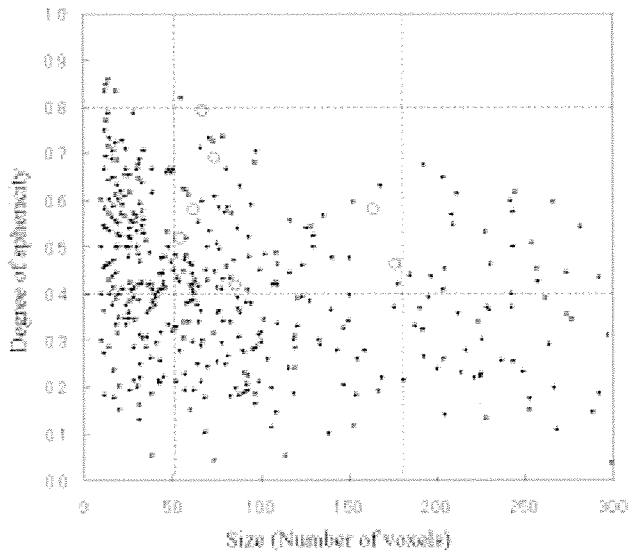

Fig.3. Relationship between size and mean value of gradient concentrate image in each of initial candidate regions (aneurysms: circles; false positive: pluses). The dotted lines indicate thresholds for removal of false positives.

III. Results

The computerized scheme for detection of intracranial aneurysms was applied to 20 clinical cases. All of the 7 aneurysms were detected correctly with 31.8 FPs per patient at the initial identification step based on the GC filer. The result indicates that the regions of all aneurysms were segmented correctly by use of our method for extracting vessel regions in the pre-processing, because the GC filter was applied to the regions of segmented vessel. We also found that the GC filter was useful for detection of aneurysms, because the regions of aneurysms have a high value in the GC images. However, a lot of FPs were remained at the initial step.

For removal of these FPs, we used three image features, i.e., size, degree of sphericity, and mean value of GC image, which were obtained from each of initial aneurysm candidates. Fig.2 shows the relationship between size and degree of sphericity. The circles and dots indicate aneurysms and FPs, respectively. As shown in this figure, the sizes of some FPs were smaller or larger than those of aneurysms, and some FPs were less circular compared with aneurysms. Thus, the size and the degree of sphericity were useful features for distinction between aneurysm and FPs. However, some FPs whose sizes were small have high values in the degree of sphericity, because it is difficult to quantify the shape of surface accurately when the size of candidate was small. Fig.3 shows the relationship between size and mean value of GC image. The mean value of GC image was useful for eliminating small line-like FPs. We applied the rules indicating the dotted lines in Fig.2 and Fig.3 to the initial candidates. As the result, 91% FPs were eliminated with the rule-based scheme.

In the final step, the quadratic discriminant analysis with three features was applied for further removal of FPs. As the result, all of the 7 aneurysms were detected correctly with 1.85 FPs per patient. Fig.4 shows the FROC curve for overall performance of our CAD scheme in detection of intracranial aneurysms on MRA images. The FROC curve was made by changing the threshold level of decision boundary. As shown in the FROC curve, the sensitivity decreased rapidly with lower FP rate. Thus, it is difficult for further removal of FPs by use of these three features. Fig.5 shows 4 aneurysms and 4 FPs, which were obtained from the final results as examples. We found that these FPs were difficult cases for distinction between aneurysms. Therefore, it may be needed other features or methods in the further work.

IV. Discussion

Because our database was small data set, same data was used for training and testing in the evaluation of the overall performance of our CAD scheme. Therefore, we need to evaluate our CAD scheme with large data set in the further study. Furthermore, since our cases were selected from one hospital, we need to collect many cases acquired from different MRA scanners in other hospitals for clinical application.

In addition, we need to conduct an observer performance study for detection of aneurysms without and with the computer output indicating the location of

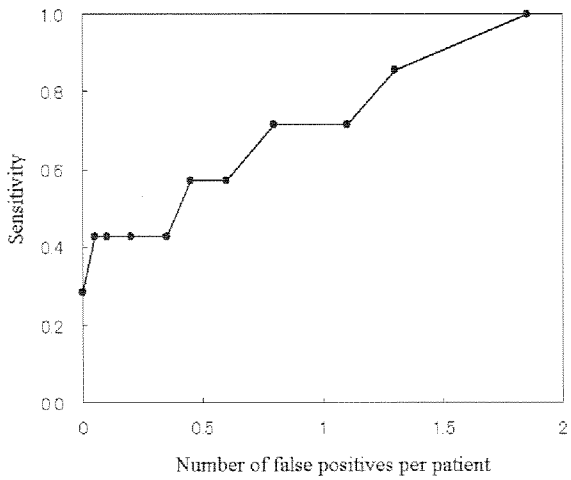

Fig.4. FROC curve for overall performance of our CAD scheme in detection of intracranial aneurysms on MRA images.

aneurysms in order to investigate whether radiologists' performance is improved or not. This result will indicate that radiologists are able to use the computer output as a second opinions to improve their diagnostic accuracy.

V. Conclusion

We have development a CAD scheme for detection of unruptured intracranial aneurysms in MRA images. With our CAD scheme, the sensitivity of the detection of aneurysms was 100% (7/7) with 1.85 FPs per patient. Therefore, this computerized scheme may be useful for radiologists in detecting unruptured intracranial aneurysms in MRA images. In our study with small data sets consisted of 20 clinical cases, we found that GC features are useful for distinction between normal vessels and aneurysms. However, further studies are required by use of large data sets to evaluate our computerized method.

Acknowledgment

The authors thank Satoshi Kasai, Ph.D., Akiko Kano, Ph.D., Hitoshi Yoshimura, Hitoshi Futamura, at Konica Minolta Medical & Graphic, Inc., Yoshinori Hayashi, Masakatsu Kakogawa, at TAK CO., Ltd., Xiangrong Zhou, Ph.D., Toshiaki Nakagawa, Ph.D., Daisuke Fukuoka, Ph.D., Yuji Hatanaka, Ph.D., and Tomoko Matsubara, Ph.D. for their valuable suggestions. The authors also thank the members of Fujita Laboratories in the Department of Intelligent Image Information, Graduate School of Medicine, Gifu University, Japan.

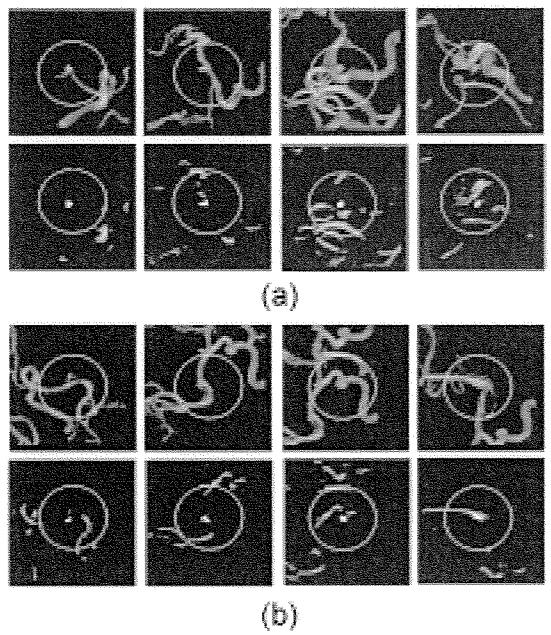

Fig.5 Illustration of (a) intracranial aneurysms and (b) false positives. The aneurysms and false positives are located in the center of each image. The top and third rows show the output images of gradient concentrate filter. The second and fourth rows show the results of our computerized method. The regions of gray color are initial aneurysm candidates. The regions of white color are the output of removal of false positives.

References

[1] J. M. Wardlaw, P. M. White, "The detection and management of unruptured intracranial aneurysms," Brain, 123, pp. 205–221, 2000.

[2] H. Arimura, Q. Li, Y. Korogi, T. Hirai, H. Abe, Y. Yamashita, S. Katsuragawa, R. Ikeda, and K. Doi, "Development of CAD scheme for automated detection of intracranial aneurysms in magnetic resonance angiography," 18th International Congress of CARS-Computer Assisted Radiology and Surgery (Chicago, USA), ICS 1268, pp. 1015-1020, 2004.

[3] H. Arimura, Q. Li, Y. Korogi, T. Hirai, H. Abe, Y. Yamashita, S. Katsuragawa, R. Ikeda, and K. Doi, "Automated computerized scheme for detection of unruptured intracranial aneurysms in three-dimensional MRA," *Academic Radiology*, vol. 11, no. 10, pp. 1093–1104, 2004.

[4] S. Rohde, K. Lahmann, J. Beck, R. Nafe, B. Yan, A. Raabe, and J. Berkefeld, "Fourier analysis of intracranial aneurysms: towards an objective and quantitative evaluation of the shape of aneurysms," *Neuroradiologyy*, vol. 47, pp. 121–126, 2005.

[5] H. Kobatake, M. Murakami, "Adaptive filter to detect rounded convex regions: iris filter," in *Proc. of International Conference on Pattern Recognition. Vol. 2. Piscataway, NJ: Institution of Electrical and Electronic Engineers*, pp. 340–344, 1996.

[6] H. Yoshida, B. Keserci, "Bayesian wavelet snake model for computer-aided diagnosis of lung nodule," *J Integrated Computer-aided Engineering* , vol. 7, pp. 253–269, 2000.

[7] J. Nappi, H. Yoshida, "Automated Detection of Polyps with CT Colonography: Evaluation of Volumetric Features for Reduction of False-Positive Finding," *Academic Radiology*, vol. 9, no. 4, pp. 386–397, 2002.

[8] K. Fukunaga "Introduction to Statistical Pattern Recognition," San Diego: Academic Press, 1990.